Supplement of Atmos. Meas. Tech., 18, 3425–3451, 2025
https://doi.org/10.5194/amt-18-3425-2025-supplement

Atmospheric Measurement Techniques
Open Access

Supplement of

Accuracy of tracer-based methane flux quantification: underlying impact of calibrating acetylene measurements

Adil Shah et al.

Correspondence to: Adil Shah (adil.shah@lsce.ipsl.fr)

S1 Picarro G2203 raw methane mole fraction calibration

The Picarro G2203 measures $[CH_4]_r$ alongside $[C_2H_2]_r$. These $[CH_4]_r$ measurements may be useful when using this gas analyser during an acetylene tracer release downwind of a methane source, rather than relying on a separate methane gas analyser. To evaluate the quality of Picarro G2203 $[CH_4]_r$ measurements, a methane calibration was conducted. This used calibrated $[CH_4]$ measurements from the Picarro G2401 as a reference. Measurements from the test to characterise MFC blending performance (used to derive C_{MFC} values corresponding to each MFC $[C_2H_2]_t$ level) were used from **Sect. 2**. Picarro G2203 $[CH_4]_r$ measurements from this test, shown in **Fig. S1**, were compared to corresponding calibrated Picarro G2401 $[CH_4]$ measurements (which are shown in **Fig. 5** (a)). For both datasets, a 5-minute average Picarro G2203 $[CH_4]_r$ and calibrated Picarro G2401 $[CH_4]$ value was taken from towards the end of each 15-minute sampling step. However, for each 60-minute $[CH_4]_0$ sampling period, a 30-minute average was used. These averages are compared in **Fig. S2**. A linear regression was applied, yielding a gain factor of 1.00807 and an offset of −0.00398 ppm, with a RMSE of ±0.000274 ppm. Although a more accurate fit may be obtained by directly sampling reference gas standards, a calibrated Picarro G2203 $[CH_4]_r$ measurement is not the objective of this work. This secondary calibration is sufficient to demonstrate the excellent capability of the Picarro G2203 to measure $[CH_4]$, even when using raw uncalibrated measurements.

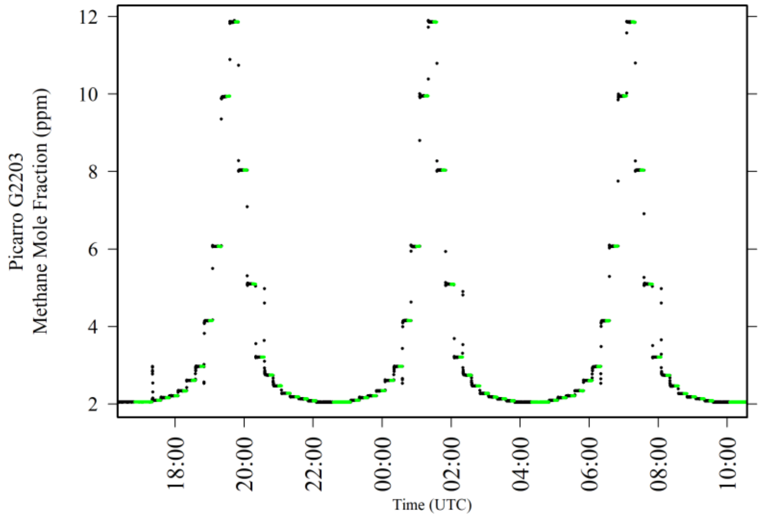

Figure S1: Picarro G2203 $[CH_4]_r$ plotted as black dots, derived from three testing cycles by blending gas from the methane calibration cylinder with natural ambient compressed air. Periods used to derive averages are highlighted as green dots.

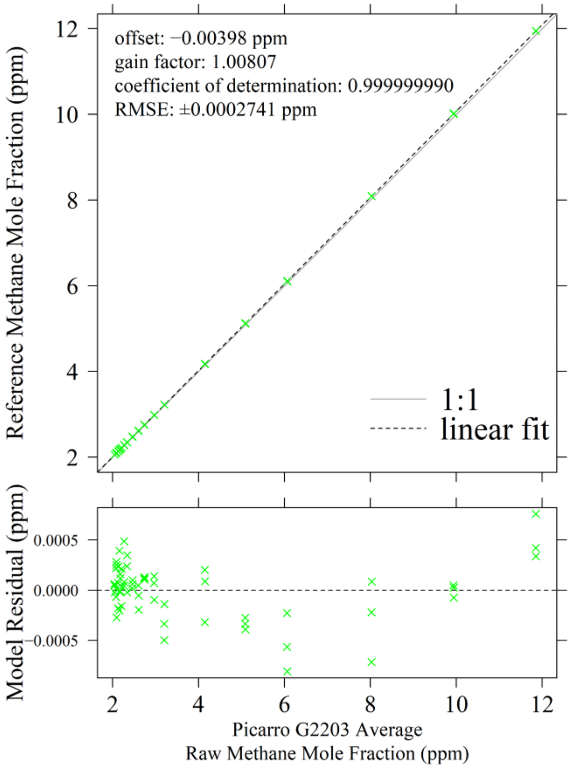

Figure S2: Top: Picarro G2203 5-minute average $[CH_4]_r$ measurements, when combining gas from the methane calibration cylinder with natural ambient compressed air, plotted against reference Picarro G2401 $[CH_4]$ levels (green crosses), with a linear regression model shown as a dashed black line and an identity line shown as a solid light-grey line. Bottom: corresponding model residuals between Picarro G2203 $[CH_4]_r$ and reference Picarro G2401 $[CH_4]$ (green crosses), with a 0 ppm $[CH_4]$ residual shown as a horizonal dashed black line.

S2 Effect of Synflex 1300 tubing on acetylene mole fraction

All laboratory testing was conducted using Synflex 1300 tubing. However, this tubing contains a low-density polyethylene coating which may interact with acetylene. To identify any potential interaction of this material with acetylene, gas from the acetylene calibration cylinder was blended with gas from a natural ambient compressed air cylinder, by connecting each gas source to a MFC. The acetylene calibration cylinder was connected to its downstream MFC using SS tubing with an OD of 0.125 inches. The gas blend from the two MFCs was connected to the Picarro G2203 either using a short length of SS tubing with an OD of 0.125 inches or using approximately 23 m of Synflex 1300 tubing with an OD of 0.25 inches, in intervals of roughly 1 hour; gas passed through each stream twice. $[C_2H_2]_r$ measurements from this test are illustrated in **Fig. S3**. A 30-minute $[C_2H_2]_r$ average was taken from towards the end of each 1-hour sampling period. $[C_2H_2]_r$ was on average (269.2±0.5) ppb and (269.4±0.5) ppb when passing though the SS line. $[C_2H_2]_r$ was on average (269.5±0.9) ppb and (269.1±0.5) ppb when passing though the Synflex 1300 line. This therefore shows that there is no noticeable difference in

$[C_2H_2]_r$ measurements when passing through Synflex 1300 tubing compared to SS tubing. Although SS may also interact with acetylene, it is highly unlikely that any artefact associated with SS would be almost identical to that of Synflex 1300.

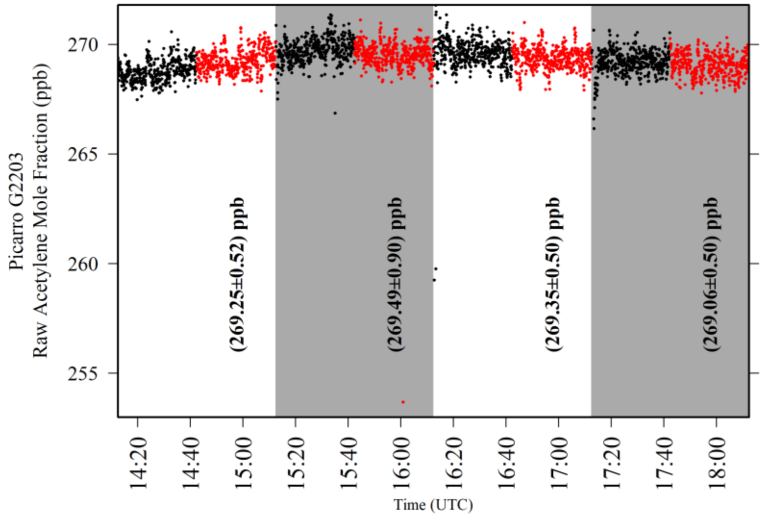

Figure S3: Picarro G2203 $[C_2H_2]_r$ plotted as black dots when sampling a fixed $[C_2H_2]$ level by blending gas from the acetylene calibration cylinder with natural ambient compressed air. Periods when gas passed through Synflex 1300 tubing are indicated as light-grey shaded periods. Periods used to derive averages are highlighted as red dots. A 30-minute average and standard deviation $[C_2H_2]_r$ measurement is shown on the plot, corresponding to gas being sampled when passing through each stream. The $[C_2H_2]_r$ plot range on the vertical axis corresponds to the range measured during 30-minute averaging periods.

S3 Raw acetylene mole fraction artefact due to humidifying and drying gas

During calibration testing to derive $[C_2H_2]$ from $[C_2H_2]_r$ (including the derivation of C_{MFC} factors used to convert $[C_2H_2]_t$ into $[C_2H_2]$ reference standards), the dew-point generator was used to humidify the gas stream which was then dried using the Nafion-based gas dryer, followed by additional drying with the magnesium perchlorate scrubber. Calibration was conducted in this way to capture any potential artefacts due to use of the Nafion-based gas dryer in conjunction with the magnesium perchlorate scrubber during field sampling. However, this assumes that the dew-point generator does not itself cause any artefacts, with it being absent in the field. Yet, use of a dew-point generator may be concerning due to the relatively high solubility of acetylene in water (Priestley and Schwarz, 1940); gas bubbles through the water reservoir of the dew-point generator during humidification making it easy for acetylene gas exchange to take place. Therefore, the effect on $[C_2H_2]_r$ measurements of using the dew-point generator, in conjunction with the Nafion-based gas dryer and the magnesium perchlorate scrubber, was tested. It was not possible to test the effect of the Nafion-based gas dryer independently of the dew-point generator as it requires wet sampling gas to operate normally.

During this test, gas from a compressed air cylinder was blended with gas from the acetylene calibration cylinder to four $[C_2H_2]_t$ settings in 15-minute steps, as illustrated in **Fig. S4**. At each $[C_2H_2]_t$ level, both pure gas was sampled from the gas blend (which is naturally dry) as well as sampling the same gas blend which was humidified and dried. Two three-way ball values were used to manually alternate between the two gas streams. A 5-minute average $[C_2H_2]_r$ measurement was taken at the end of each 15-minute sampling period, which is given in **Fig. S4**, alongside its standard deviation variability. These results show that the two gas streams produced identical $[C_2H_2]_r$ measurements, within the bounds of uncertainty. This confirms that the combined effect of using the dew-point generator, the Nafion-based gas dryer and the magnesium perchlorate scrubber has no significant effect on $[C_2H_2]$, compared to sampling pure dry gas without humidification and drying.

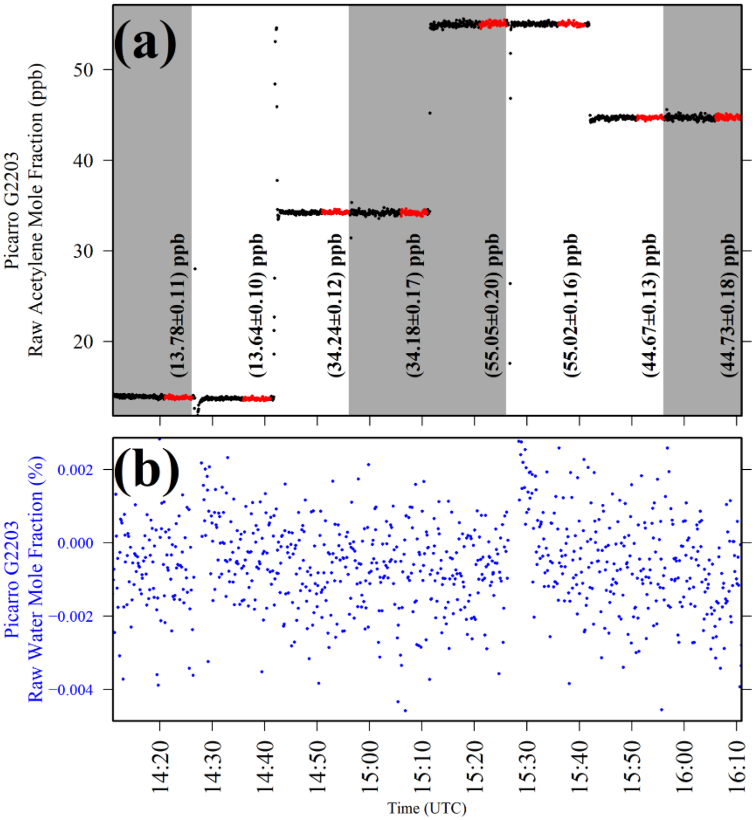

Figure S4: (a) Picarro G2203 $[C_2H_2]_r$ plotted as black dots and (b) Picarro G2203 $[H_2O]_r$ plotted as blue dots, when sampling four different $[C_2H_2]_t$ settings by blending gas from the acetylene calibration cylinder with natural ambient compressed air. At each $[C_2H_2]_t$ setting, pure dry gas was sampled (light-grey shaded periods in (a)) as well as sampling gas passing through the dew-point generator, the Nafion-based gas dryer and the magnesium perchlorate scrubber (unshaded periods in (a)). Periods used to derive averages are highlighted as red dots in (a). A 5-minte average and standard deviation $[C_2H_2]_r$ measurement is shown on the plot for each $[C_2H_2]_t$ setting, corresponding to gas being sampled when passing through each stream in (a). The $[C_2H_2]_r$ and $[H_2O]_r$ plot range in (a) and (b), respectively, correspond to the range measured during 5-minute averaging periods.

S4 Picarro G2401 water mole fraction during water characterisation tests

The effect of $[H_2O]_r$ changes on Picarro G2203 $[C_2H_2]_r$ measurements was tested at nine different $[C_2H_2]_r$ levels in **Sect. 2**. During this test, erratic Picarro G2203 $[H_2O]_r$ measurements were occasionally observed. However, simultaneous measurements made by the Picarro G2401 gas analyser, measuring the same gas stream, did not observe erratic $[H_2O]_r$ measurements, as illustrated in **Fig. S5**. This therefore confirms that erratic Picarro G2203 $[H_2O]_r$ measurements are an artefact of the Picarro G2203 gas analyser, rather than due to the contents of the gas mixture.

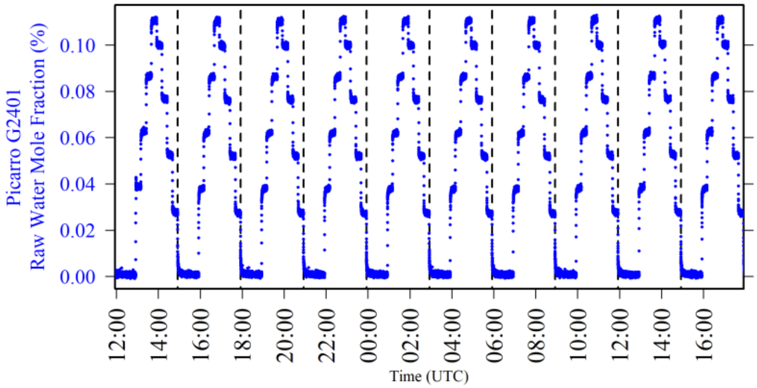

Figure S5: Picarro G2401 $[H_2O]_r$ plotted as blue dots when sampling nine different low $[H_2O]$ levels at five different $[C_2H_2]_t$ settings over two testing cycles, with the change between each different $[C_2H_2]_t$ setting indicated by dashed vertical lines.

S5 Effect of uncertainties in cylinder supplier mole fractions on acetylene calibration

The overall acetylene calibration procedure for the Picarro G2203 presented in **Sect. 2** relies on both the declared $[CH_4]$ level in the methane calibration cylinder and the declared $[C_2H_2]$ level in the acetylene calibration cylinder. Neither of these values is certified using reference standards and each mole fraction is associated with an uncertainty declared by the cylinder provider (±0.5% for the methane calibration cylinder and ±3% for the acetylene calibration cylinder). The declared $[CH_4]$ level is used to derive $[CH_4]_t$ values which are therefore used to derive C_{MFC} values corresponding to each $[C_2H_2]_t$ setting (*i.e.* each MFC dilution blending setting). Meanwhile the declared $[C_2H_2]$ level is used to determine each $[C_2H_2]_t$ value which, in conjunction with C_{MFC}, is used to derive standard reference $[C_2H_2]$ levels for Picaro G2203 calibration, through comparison against $[C_2H_2]_r$ measurements. This analysis tests the influence of these declared cylinder uncertainty ranges on the Picarro G2203 acetylene calibration.

First, the range in possible $[CH_4]_t$ values at each MFC setting was calculated, due to the uncertainty in the declared $[CH_4]$ of the methane calibration cylinder. For each $[CH_4]_t$ range, corresponding C_{MFC} values were derived using Eq. **(2)** following the same procedure described in **Sect. 2**. These $[CH_4]_t$ and C_{MFC} ranges are illustrated in **Fig. S6**, which show that maximising $[CH_4]_t$ (*i.e.* using the upper uncertainty range of the methane calibration cylinder declared $[CH_4]$ level) minimises C_{MFC} at each MFC setting and *vice versa*. Next, the range in possible $[C_2H_2]_t$ values at each MFC setting was calculated, due to the uncertainty in the declared $[C_2H_2]$ of the acetylene calibration cylinder. For each $[C_2H_2]_t$ range, a range in possible $[C_2H_2]$ standard reference levels was calculated using Eq. **(1)** following the same procedure described in **Sect. 2**, where the upper limit of each $[C_2H_2]_t$ range was combined with the minimum C_{MFC} value at each MFC setting (to maximise $[C_2H_2]$ reference levels) and *vice versa*. This range in [C_2H_2] values at each MFC setting was used to derive different Picarro G2203 [C_2H_2]$_r$ calibration fits, as illustrated in **Fig. S7**, for MFC settings corresponding to each [C_2H_2] level except the lowest four. This shows that maximised standard [C_2H_2] values result in a gain factor of 0.977 and an offset of −0.152 ppb, while minimised standard [C_2H_2] values result in a gain factor of 0.911 and an offset of −0.142 ppb.

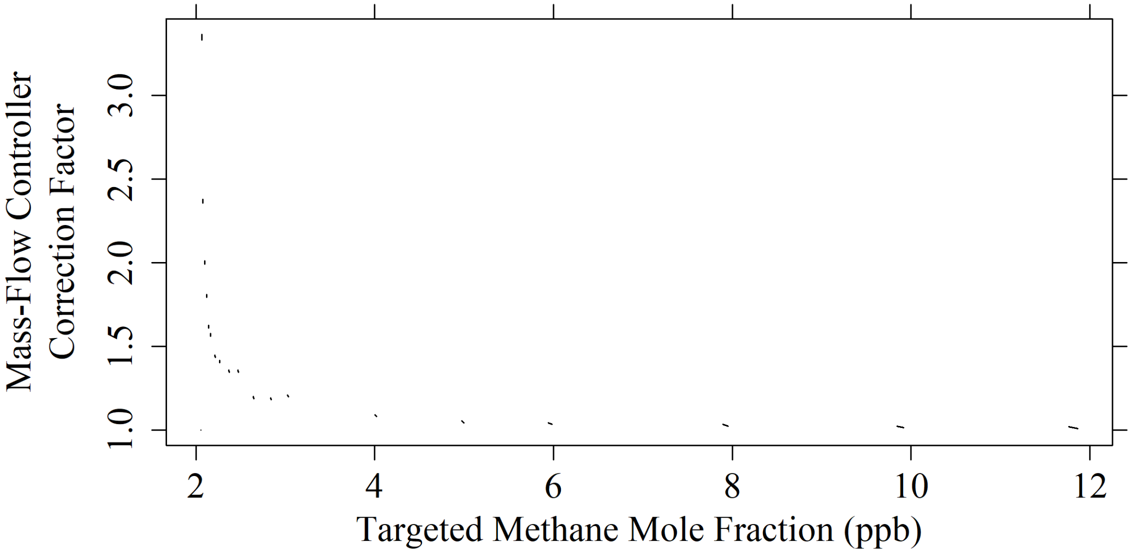

Figure S6: The range in calculated [CH_4]$_t$ values at each MFC setting, plotted as black lines on the horizontal axis, when blending gas from the methane calibration cylinder with natural ambient compressed air, derived across the full uncertainty range of the declared [CH_4] level of the methane calibration cylinder. The vertical component of each line shows the range in C_{MFC} values corresponding to the range in calculated [CH_4]$_t$ values at each MFC setting, derived using Eq. (2) in conjunction with the average of [CH_4] measurement averages from three testing cycles.

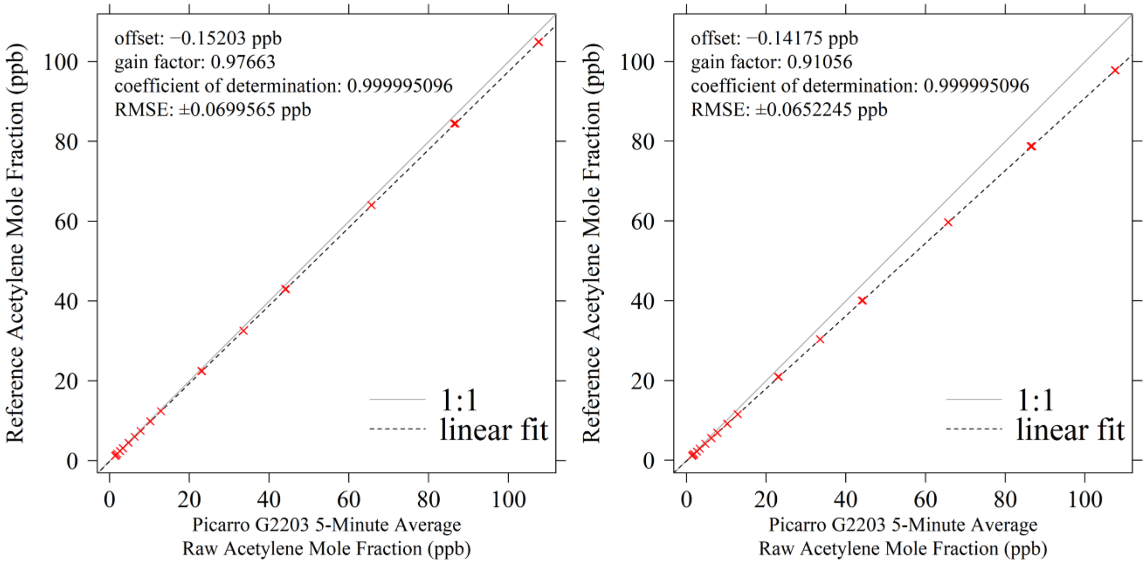

Figure S7: Picarro G2203 5-minute average $[C_2H_2]_r$ measurements, when combining gas from the acetylene calibration cylinder with natural ambient compressed air, plotted against maximised (right) and minimised (left) reference $[C_2H_2]$ levels (red crosses), with a linear regression model shown as a dashed black line and an identity line shown as a solid light-grey line. Maximised reference $[C_2H_2]$ levels were derived using the upper declared $[C_2H_2]$ uncertainty bound of the acetylene calibration cylinder and the lower declared $[CH_4]$ uncertainty bound of the methane calibration cylinder. Minimised reference $[C_2H_2]$ levels were derived using the lower declared $[C_2H_2]$ uncertainty bound of the acetylene calibration cylinder and the upper declared $[CH_4]$ uncertainty bound of the methane calibration cylinder.

S6 Unstable low Picarro G2203 raw acetylene mole fraction measurements

When sampling at $[C_2H_2]$ levels of less than 1.16 ppb, the Picarro G2203 reported unstable $[C_2H_2]_r$ measurements that occasionally resolved to the $[C_2H_2]_r$ level observed at 0 ppb $[C_2H_2]$. An example of this is given in **Fig. S8** when gas from the acetylene calibration cylinder was blended with compressed ambient air to sample an $[C_2H_2]$ of 0.349 ppb, following a direct transition from sampling an $[C_2H_2]$ of 0.867 ppb. The data presented in **Fig. S8** is a subset of the data presented in **Fig. 6** (a).

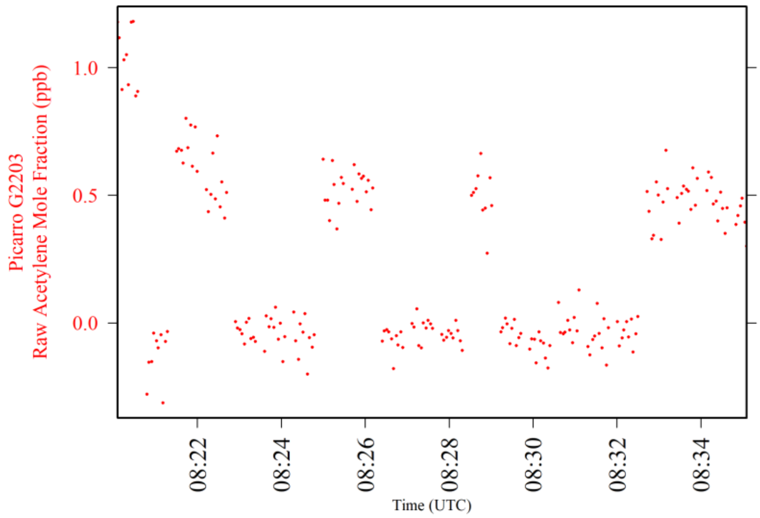

Figure S8: Picarro G2203 $[C_2H_2]_r$ plotted as red dots, starting with the transition from sampling an $[C_2H_2]$ of 0.867 ppb to sampling an $[C_2H_2]$ of 0.349 ppb by blending gas from the acetylene calibration cylinder with natural ambient compressed air.

S7 Acetylene calibration using zero-air generator gas for dilution

An acetylene calibration was conducted using the same $[C_2H_2]_t$ range from **Sect. 2** (corresponding to the same MFC settings), but using gas from the zero-air generator for dilution, instead of gas from a natural ambient compressed air cylinder. The zero-air generator was supplied with compressed ambient outdoor air as gas input. It catalytically and thermally oxidises hydrocarbons and carbon monoxide, resulting in a $[CH_4]_0$ of 0 ppm and $[C_2H_2]_0$ of 0 ppb in the gas output. A similar overall set-up was used as illustrated schematically in **Fig. 4**, but the natural ambient air cylinder was replaced with the zero-air generator source. An additional diaphragm pump was placed downstream of the zero-air generator to pressurise gas flow, with an upstream vent to maintain atmospheric pressure upstream of the pump. For this test, new C_{MFC} values were derived to account for any differences due to MFC performance over time and in the different conditions. Twenty different $[CH_4]_t$ levels between $[CH_4]_0$ and 9.78 ppm were targeted in the same way with the same MFC settings as when diluting gas from the methane calibration cylinder with natural ambient compressed air, as described in **Sect. 2**. Calibrated $[CH_4]$ measurements from the Picarro G2401 were averaged in the same way as described in **Sect. 2**, to derive C_{MFC} values using Eq. **(2)**, which are presented in **Fig. S9**. This enabled $[C_2H_2]$ standards to be derived from $[C_2H_2]_t$. using Eq. **(1)**. Next, the same MFC blending procedure was performed, but instead using the acetylene calibration cylinder in place of the methane calibration cylinder, to sample twenty different $[C_2H_2]$ levels between $[C_2H_2]_0$ and 101.6 ppm, as shown in **Fig. S10**. The same averaging was performed on this dataset as discussed in **Sect. 2**. Averages made at the four lowest $[C_2H_2]$ levels were excluded from the calibration, following **Sect. 2**, due to unstable Picarro G2203 $[C_2H_2]_r$ measurements at low $[C_2H_2]$ levels. A linear regression was applied to the remaining data, as illustrated in **Fig. S11**, yielding a gain factor of 0.9413 and an offset of +0.0139 ppb, with a RMSE of ±0.0356 ppb.

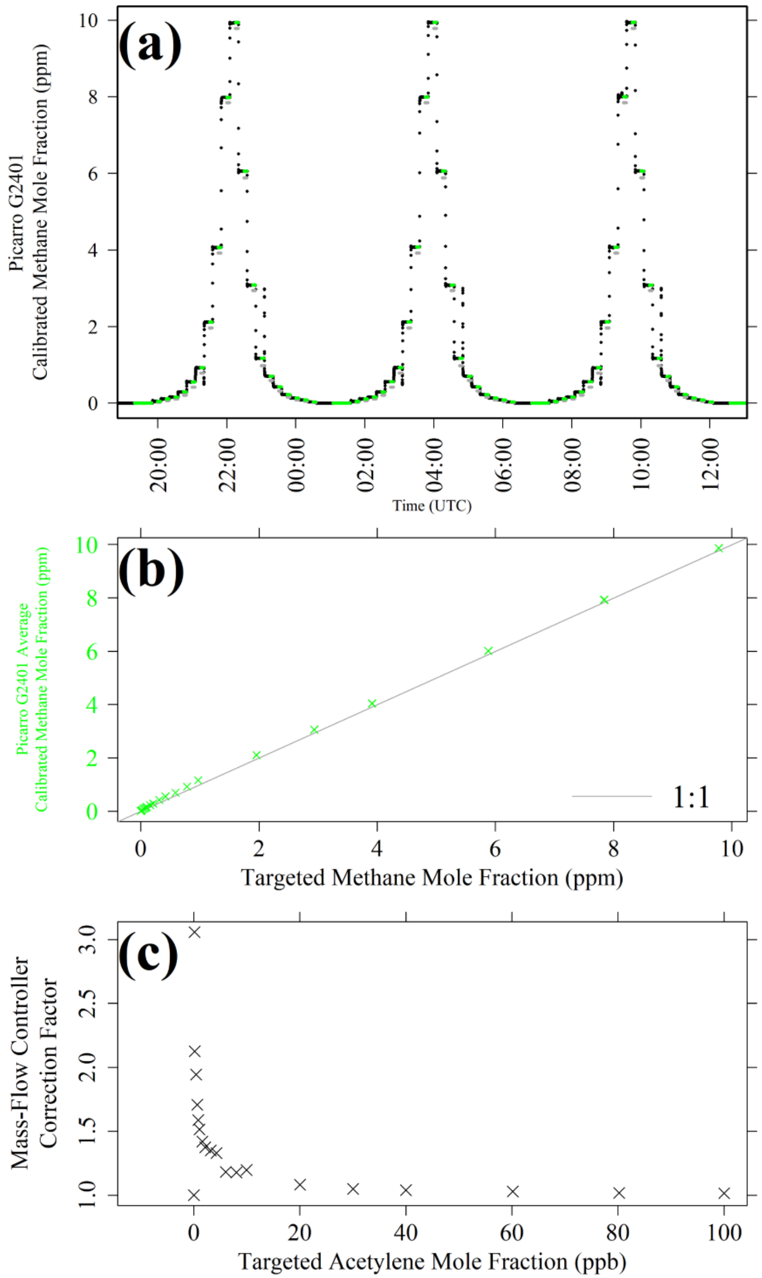

Figure S9: (a) Picarro G2401 $[CH_4]$ plotted as black dots, (b) corresponding $[CH_4]$ 5-minute averages plotted as green crosses against calculated $[CH_4]_t$ and (c) C_{MFC} as a function of corresponding calculated $[C_2H_2]_t$ levels, derived from three testing cycles by blending gas from the methane calibration cylinder with gas from a zero-air generator. Periods used to derive averages are highlighted as green dots and corresponding calculated $[C_2H_2]_t$ levels are shown in the background as light-grey dots in (a). An identity line is shown as a solid light-grey line in (b).

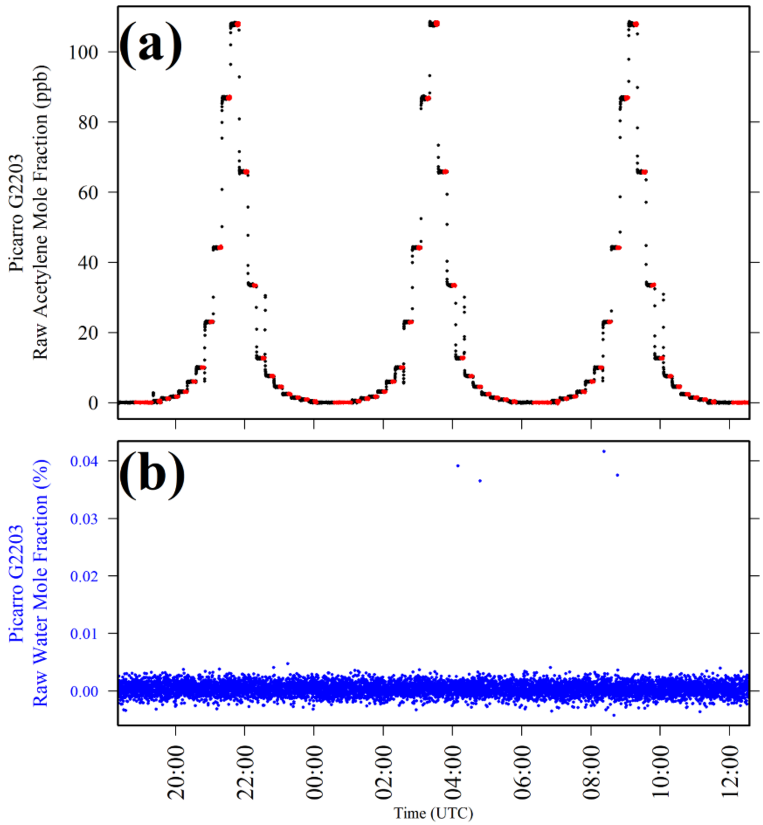

Figure S10: (a) Picarro G2203 $[C_2H_2]_r$ plotted as black dots and (b) Picarro G2203 $[H_2O]_r$ plotted as blue dots, when sampling twenty different standard $[C_2H_2]$ levels over three testing cycles by blending gas from the acetylene calibration cylinder with gas from a zero-air generator. Periods used to derive averages are highlighted as red dots in (a).

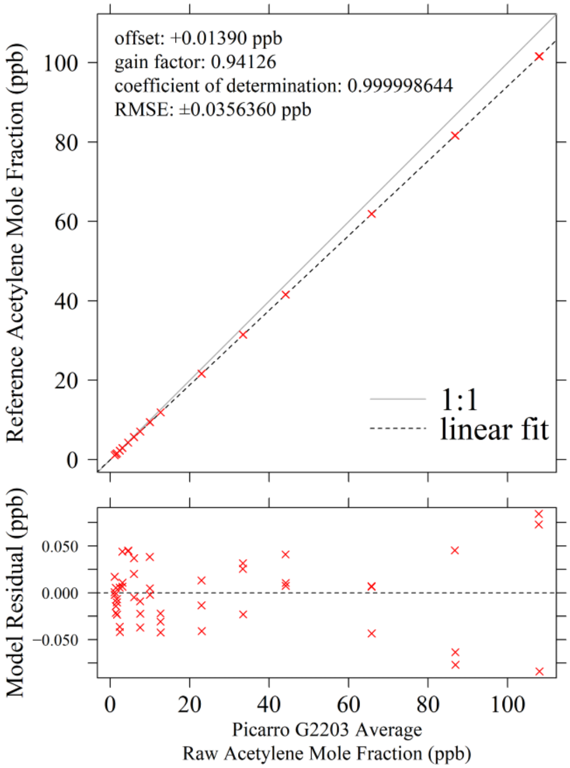

Figure S11: Top: Picarro G2203 5-minute average $[C_2H_2]_r$ measurements, when combining gas from the acetylene calibration cylinder with gas from the zero-air generator, plotted against reference $[C_2H_2]$ levels (red crosses), with a linear regression model shown as a dashed black line and an identity line shown as a solid light-grey line. Bottom: corresponding model residuals between $[C_2H_2]_r$ and $[C_2H_2]$ (red crosses), with a 0 ppb $[C_2H_2]$ residual shown as a horizonal dashed black line.

S8 Measurement stability at an acetylene mole fraction of 0 ppb

The stability of Picarro G2203 acetylene measurements when sampling an $[C_2H_2]$ of 0 ppb was assessed by performing an additional σ_A^2 test to that presented in **Sect. 2** (which was conducted at an $[C_2H_2]$ of 10.1 ppb). Pure gas from a natural ambient compressed air cylinder was sampled for 12 hours, corresponding to an $[C_2H_2]$ of 0 ppb. A modified version of the set-up illustrated schematically in **Fig. 4** was used to save gas, as no dilution is required; the compressed air cylinder was connected directly to a single MFC, before subsequent humidification and drying. $[C_2H_2]_r$ measurements were corrected by subtracting a fixed offset value of 0.012 ppb, as the linear model calibration fit presented in **Sect. 2** is not valid below 1.16 ppb $[C_2H_2]$ (although, in theory, this offset correction has no effect in this analysis on variance). An σ_A^2 test was conducted using subsets of the prolonged dataset, with the σ_A^2 test repeated ten times to obtain average of σ_A^2 values and corresponding integration times, using the same procedure described in **Sect. 2**.

A logarithmic plot showing σ_A at 0 ppb $[C_2H_2]$ as a function of integration time is given in **Fig. S12**, with a white noise line also shown. The σ_A at the smallest integration time is ±0.0577 ppb (4.24 s integration time). While **Fig. S12** shows generally decreasing σ_A with integration time, as expected, an interesting feature occurs in the first 100 s where σ_A increases slightly before continuing its decline as a function of integration time, following a trend close to the white noise line (although offset from σ_A at the lowest integration time). This could be associated with the roughly 40 s $[C_2H_2]_r$ measurement cycle, with the Picarro G2203 consistently struggling to fit for an absence of acetylene over each of the ten samples. The difference between the **Fig. 8** ($[C_2H_2]$ of 10.1 ppb) and **Fig. S12** ($[C_2H_2]$ of 0 ppb) fits supports the suggestion from **Sect. 2**, that the Picarro G2203 $[C_2H_2]$ response is different at very low $[C_2H_2]$ levels, close to 0 ppb. Nevertheless, this σ_A^2 test at an $[C_2H_2]$ of 0 ppb shows no clear sustained inflection in σ_A decrease with integration time.

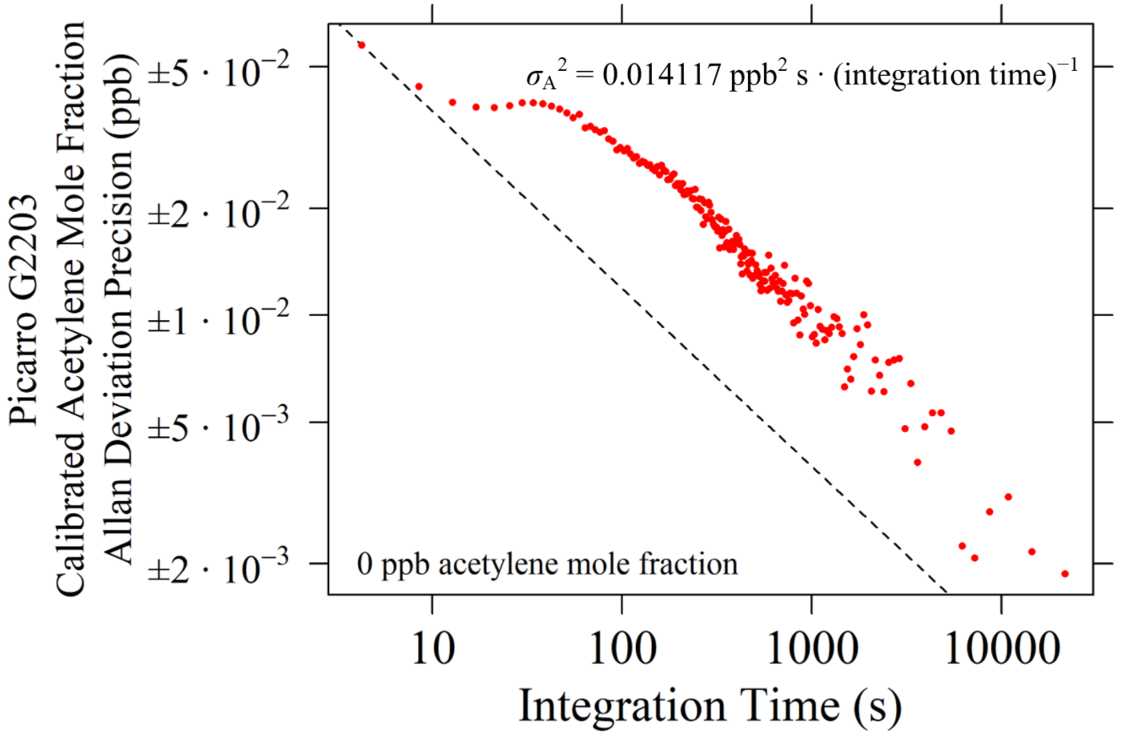

Figure S12: σ_A for Picarro G2203 calibrated $[C_2H_2]$ measurements as a function of integration time derived from an average of ten different tests, plotted as red dots, when sampling an $[C_2H_2]$ of 0 ppb. Logarithmic axes are used. The black dashed line depicts white noise, with this fit forced to intersect with σ_A at the lowest integration time (the fitting coefficient is provided inside the plot).

S9 Acetylene flow meter

The acetylene flow meter uses the Coriolis technique to measure gas flow, as described in detail by Baker (2016). It can measure up to a maximum $Q_{acetylene}$ of 8.67 g s^{-1} at 288.15 K under a gauge pressure of 1 bar, with maximum measurable $Q_{acetylene}$ increasing with absolute pressure. The acetylene flow meter has been factory calibrated using rigs traceable to

ISO 17025, with error limits based on ISO 11631. It requires a direct current power supply of between 19 V and 29 V, which is provided by converting the output from a 12 V lithium ion phosphate battery up to 24 V.

During field operation, $Q_{\text{acetylene}}$ can be viewed on a display interface. A current loop also outputs analogue $Q_{\text{acetylene}}$ data within a range of between 4 mA and 20 mA; this output is connected to an analogue current to voltage converter (SEN0262, Zhiwei Robotics Corp, Shanghai, China). The voltage output from the analogue current to voltage converter is connected to an analogue to digital converter chip (MCP3424, Microchip Technology Inc., Chandler, Arizona, USA) which is ready-mounted on a board (ADC Pi board, Apexweb Ltd, Swanage, Dorset, UK); this is connected to a logging computer (Raspberry Pi Zero W, Raspberry Pi Foundation, Cambridge, UK), which records 16 bit voltage measurements (corresponding to a 0.154 mV voltage resolution) at 1 Hz. A baseline voltage correction is applied to all voltage measurements obtained during each acetylene gas release, by applying a linear fit as a function of time to voltage measurements before and after gas release, corresponding to zero gas flow. An Internet time synchronisation proceeds any data logging on the logging computer.

The performance of the acetylene flow meter was tested by comparison with flow rate measurements made by a MFC. Compressed outdoor air supplied to our laboratory building was simultaneously sampled by both the acetylene flow meter and the MFC. The MFC used in this test has a maximum flow rate of 15 $\text{dm}^3\ \text{min}^{-1}$ at 273.15 K and 101 325 Pa when sampling dry air, which was logged at approximately 10 Hz. The MFC was fully opened, allowing unimpeded gas flow and flow measurement. The flow rate was varied in rough stages up to 0.3 g s^{-1}. The flow rate and pressure were adjusted during each stage to ensure that the gauge pressure always fell between a range of between 0.5 bar and 1.0 bar, to replicate field operation conditions described in **Sect. 3**. Other unstable transition periods led to poor correspondence between the MFC and the acetylene flow meter as the pressure was not stable and adjustments were being made; these periods were identified and excluded from the comparison. All MFC data was interpolated to the lower timestamp of the acetylene flow meter. A comparison is presented in **Fig. S13**, which shows good agreement across the tested range, with a Pearson correlation coefficient of 0.9999627. This test therefore confirms excellent correlation between the two flow rate measurements. It also confirms our ability to derive acetylene flow meter $Q_{\text{acetylene}}$ measurements from the acetylene flow meter data output current loop.

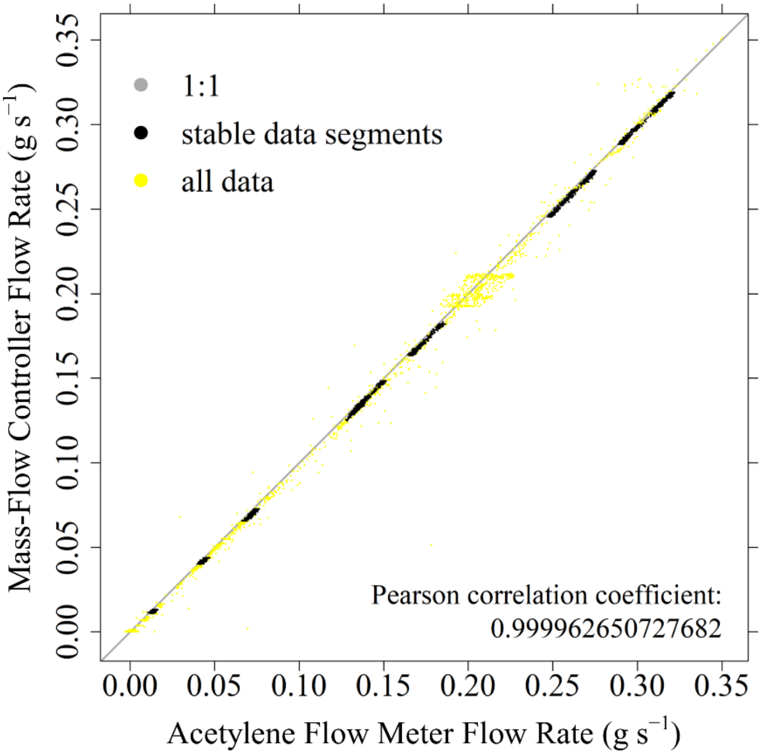

Figure S13: A comparison between $Q_{\text{acetylene}}$ measured by the acetylene flow meter (horizontal axis) and a MFC flow rate measurement (vertical axis), plotted as yellow dots. Periods of stable sampling are plotted as black dots. An identity line is shown (light-grey) in the background.

S10 Safety exclusion zone

A safety exclusion zone is designated as being 6 m away from the release point, with all acetylene release equipment placed outside of this zone. This distance is calculated such that [C_2H_2] cannot exceed its lower atmospheric flammable limit of 2.5% (Williams and Smith, 1969) considering an $Q_{\text{acetylene}}$ of 0.5 g s^{-1} (which over twice the nominal maximum safe $Q_{\text{acetylene}}$ level for the acetylene cylinder as discussed in **Sect. 3**) and using Gaussian plume modelling in the worst-case Pasquill stability class (Turner, 1994), with a mean wind speed of 0.1 m s^{-1} to accentuate [C_2H_2]. The boundaries of the safety exclusion zone are designated by cones during an acetylene release, with the zone being constantly manned by the release operator who stands outside the zone and continuously surveys the acetylene release equipment.

S11 Wind conditions and flow rate during sampling

The duration of the sampling campaign is defined as running from 08:34:06.4 (UTC) to 11:00:40.2 (UTC) on 16 February 2024, representing a total duration of 146 minutes and 33.7 s. This corresponds to the period running from

20 minutes before the start of the first transect up until the time of the end of the final transect, on the road between Point A and Point B. Sonic anemometer wind speed and wind direction measurements for the full duration of the acetylene release are presented in **Fig. S14** (b and c, respectively). Acetylene flow meter $Q_{\text{acetylene}}$ measurements are also presented in **Fig. S14** (a). Measurements in **Fig. S14** are highlighted for the full duration of the sampling campaign, as defined here.

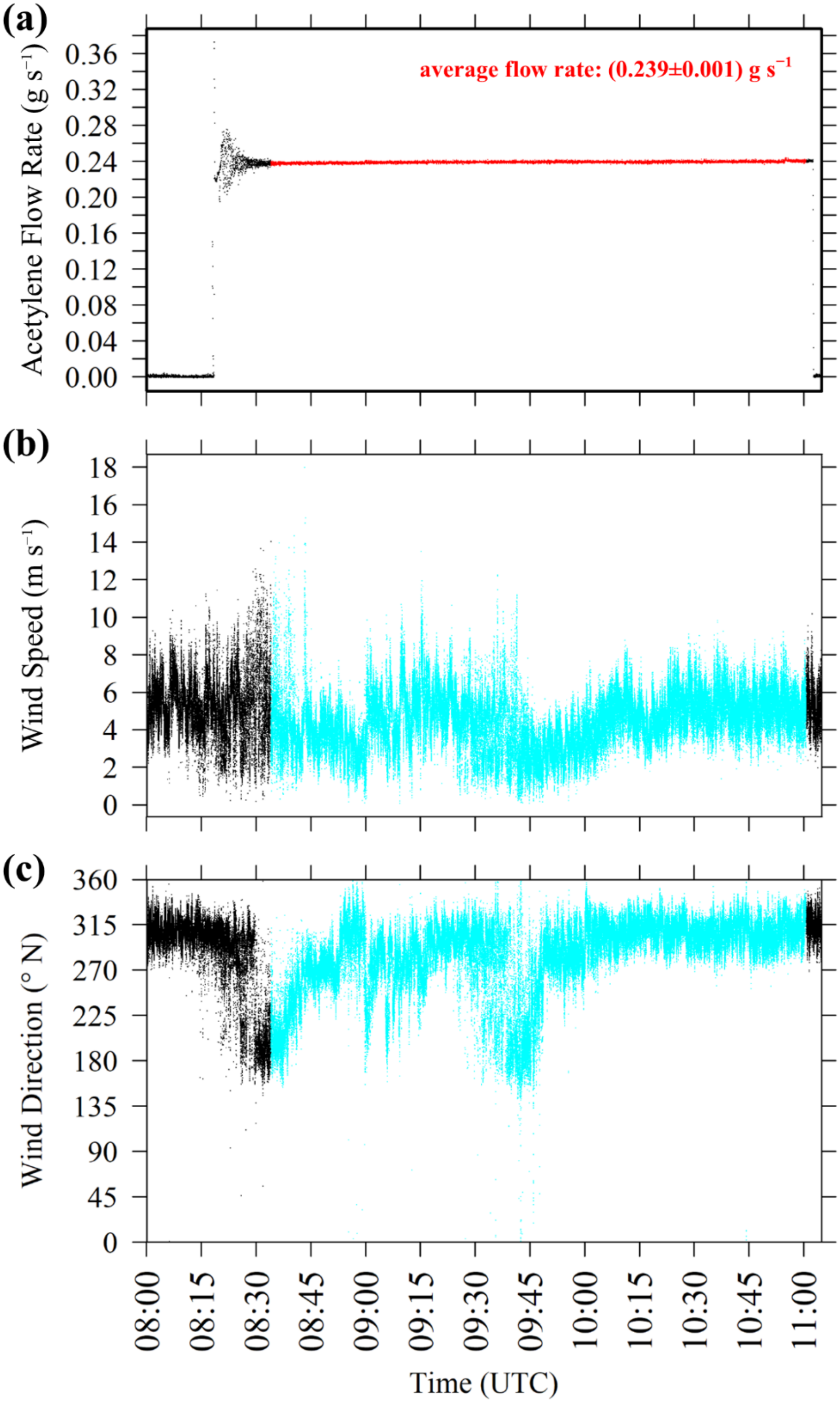

Figure S14: (a) Acetylene flow meter $Q_{acetylene}$, (b) sonic anemometer two-dimensional scalar wind speed and (c) sonic anemometer two-dimensional wind direction with respect to True North, all plotted as black dots. Periods of sampling from 20 minutes before the first transect up to the end of the final transect and shown as red dots in (a), cyan dots in (b) and cyan dots in (c).